

Sub-picosecond acoustic pulses generated at buried GaP/Si interfaces

Kunie Ishioka,^{1,*} Avinash Rustagi,² Andreas Beyer,³ Wolfgang Stolz,³
Kerstin Volz,³ Ulrich Höfer,³ Hrvoje Petek,⁴ and Christopher J. Stanton²

¹*National Institute for Materials Science, Tsukuba, 305-0047 Japan*

²*Department of Physics, University of Florida, Gainesville, FL 32611 USA*

³*Philipps-University, Material Sciences Center and Faculty of Physics, D-35032 Marburg, Germany*

⁴*Department of Physics and Astronomy, University of Pittsburgh, Pittsburgh, PA 15260, USA*

(Dated: October 25, 2018)

Photoexcitation of a lattice-matched GaP/Si(001) interface with a femtosecond laser pulse generates coherent acoustic phonons, which propagate ballistically into both GaP and Si. The acoustic pulses induce quasi-periodic modulations in the reflectivity through the photoelastic effect. When the acoustic pulse strikes the GaP/air surface, it induces surface expansion and gives rise to a ultra-short (~ 0.5 ps) spike in the reflectivity. The extremely short duration of the acoustic pulse, which corresponds to spatial extent of 3 nm, indicates that it is generated exclusively at the atomically abrupt GaP/Si interface.

I. INTRODUCTION

Coherent acoustic phonons can be generated by photoexciting metals, semiconductors and their nanostructures with ultrashort laser pulses [1]. They take the form of strain or shear pulses propagating in a bulk crystal or on a surface, as well as periodic deformations of entire nanoparticles. Ultrafast dynamics of the coherent acoustic phonons on the picosecond time scale have been studied extensively by means of time-resolved optical [2, 3] and x-ray diffraction [4] measurements. Such studies are motivated by determination of the mechanical properties of crystals and nanoparticles [5–8], ultrafast optical control of piezoelectric effect [9] and magnetism [10], development of nanoplasmonic resonators [11] and terahertz polaritonics [12].

Coherent acoustic phonons can be a useful tool also in nano-seismology and nano-tomography for characterizing buried interfaces and defective layers, objects hidden under the surfaces, molecules adsorbed on surface, local strains, *etc* [13–17]. For such applications, higher-frequency and therefore shorter-duration acoustic phonons provide better spatial resolution. The duration of the acoustic pulse is primarily determined by the absorption depth of the excitation light [1, 18] or the thickness of a metallic opto-acoustic transducer on top of a transparent crystal. One way to make ultrashort acoustic pulses is to generate surface acoustic waves (SAWs) using one- or two-dimensional metallic nano-gratings. The shortest wavelength of SAWs achieved so far was 45 nm, determined by the periodicity of the grating [19]. Another approach is to confine coherent acoustic phonon pulses into sub-micron scale objects. The shortest acoustic pulse actually measured, with a wavelength of 150 nm, was achieved by focusing an acoustic pulse inside a metal-coated silica fiber [20]. However, transferring such short

acoustic pulses into a three-dimensional crystal without increasing its wavelength has been a great challenge [21].

In the present study, we investigate the coherent acoustic phonons generated at lattice-matched GaP/Si(001) heterointerfaces. GaP can be grown with nearly perfect lattice match and without extended defects on exact Si(001) substrate. Therefore it has the potential for incorporating optical functions in Si based electronic devices as well as for high efficiency multi-junction solar cells [22]. Optical generation of intrinsic acoustic pulses in indirect band gap semiconductors GaP and Si without aid of opto-acoustic transducers has been studied recently in pump-probe reflectivity scheme [23]. In the present study we find coherent acoustic phonons generated at the GaP/Si interface with extremely short temporal (~ 0.5 ps) and spatial (~ 3 nm) widths that are generated exclusively at the GaP/Si interface, and detected at the GaP/air surface after propagating in the thin GaP layers.

II. EXPERIMENTAL METHODS

The samples studied are nominally undoped GaP films grown by metal organic vapor phase epitaxy on the *n*-type Si(001) substrates with different thicknesses from $L=16$ to 56 nm. Details of the sample preparation and the evaluation of the atomic-scale structure are described elsewhere [24]. Transmission electron microscopy (TEM) images confirm that all the GaP layers have abrupt GaP/Si interfaces and smooth surfaces, with intermixing layer of $\lesssim 7$ atomic layers [25], while the density of planar defects is minimized. The thicknesses of the GaP layers are measured by x-ray diffraction.

Pump-probe reflectivity measurements are performed in a near back-reflection configuration [Fig. 1] using laser pulses with 400-nm wavelength (3.1-eV photon energy) and 10-fs duration. Details of the measurements were described elsewhere [26]. Pump-induced change in the reflectivity ΔR is measured as a function of time delay

* ishioka.kunie@nims.go.jp

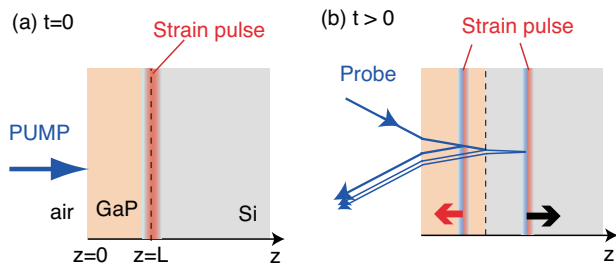


FIG. 1. (Color Online.) Schematics of the experiment. (a) At $t = 0$ pump light generates an acoustic pulse at GaP/Si interface ($z = L$). (b) The acoustic pulses propagate both in GaP and Si crystals. The probe light is reflected at the acoustic pulses as well as the surface and the interface, leading to the periodic modulation of the reflectivity. The incident angle of the probe light in (b) is exaggerated for clarity. The acoustic pulse generated at the GaP surface and the probe light paths not directly involved in the detection are left out for simplicity.

between pump and probe pulses using a fast scan technique. The optical absorption depth, $\alpha_{\text{GaP}}^{-1} = 116$ nm [27], exceeds the GaP film thicknesses ($L = 56$ nm at maximum) studied in the present study. The 3.1-eV photons are also absorbed by the Si substrate ($\alpha_{\text{Si}}^{-1} = 82$ nm).

III. EXPERIMENTAL RESULTS

Figure 2 compares the reflectivity responses from the GaP films of different thicknesses L , together with those of the bulk GaP and Si already reported in Ref. [23]. All the traces show steep rise or drop at $t=0$, followed by recovery on a time scale of 1 ps [Fig. 2b], which arise from the photoexcited carrier dynamics. The reflectivity traces are also modulated by oscillations with sub-100 fs periods and several ps dephasing times due to coherent optical phonons of GaP and Si, whose details have been reported elsewhere [28].

In the longer time scale, the reflectivity traces of the GaP/Si samples show quasi-periodic oscillations on tens of picoseconds time scale, as shown in Fig 2a. Similar but more regular oscillations are observed also for bulk GaP and bulk Si, which we attributed to an interference between the probe lights reflected from the surface and from the propagating strain pulse, also known as Brillouin oscillation, in our previous study [23]. The frequency f_B of such oscillation is given by $f_B = 2nv/\lambda = 123$ and 235 GHz for GaP and Si in the case of normal incidence, with n being the refractive index, v , the longitudinal acoustic (LA) phonon velocity, and λ , the probe wavelength [1, 23]. Fourier-transformed (FT) spectrum for the thickest ($L=56$ nm) GaP film [Fig. 2c] is dominated by a spike at f_B^{GaP} , confirming an acoustic pulse propagating in the GaP film as the main origin of the reflectivity modulation. The FT spectra for the thinner films, by contrast, have both f_{GaP} and f_{Si} components, indicating that at

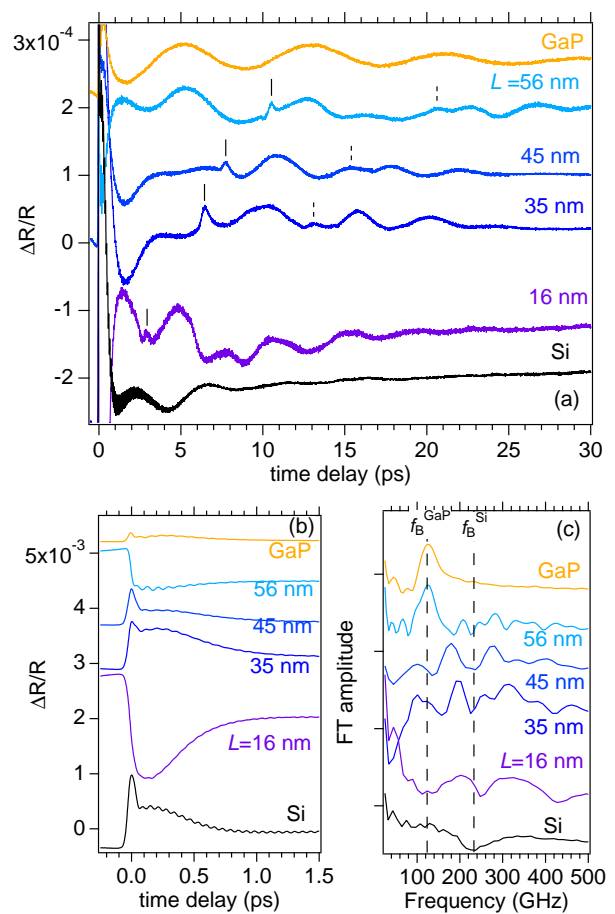


FIG. 2. (Color Online.) (a,b) Reflectivity changes of the GaP films of different thicknesses L on Si(001) substrates, together with those of bulk Si and GaP. Pump densities are $90 \mu\text{J}/\text{cm}^2$ for bulk Si and $30 \mu\text{J}/\text{cm}^2$ for other samples. (a) and (b) show identical traces with different vertical and horizontal scales. Solid and broken lines in (a) indicate the first and second reflectivity spikes. (c) Fourier-transformed spectra of the reflectivity changes for time delay $0.1 < t < 35$ ps.

least two acoustic pulses, one moving in GaP and another in Si, are contributing to the reflectivity modulation.

In addition to the quasi-periodic modulations, the reflectivity traces from the GaP/Si samples exhibit sharp spikes, whose positions are indicated by solid lines in Fig. 2a]. Such spikes are absent for bulk GaP and Si, and appear at longer time delays τ_1 for the GaP/Si samples with larger GaP film thickness L , as plotted with the filled symbols in Fig. 3a. The slope of the plot, $\tau_1/L = 0.183 \pm 0.014$ ps/nm, corresponds to the inverse group velocity of the LA phonon of GaP in the [001] direction, $v_{\text{GaP}}^{-1} = 0.1710 \times 10^{-5} \text{ cm}^{-1} \text{ s}$ [29]. The agreement between v_{GaP} and L/τ_1 , not $2L/\tau_1$, implies that the reflectivity spikes are induced by the LA phonon wave packet after traveling in the GaP film only one way. We tentatively attribute the spikes to the acoustic pulses generated at the GaP/Si interface and detected at the GaP/air surface, rather than the other way around, as

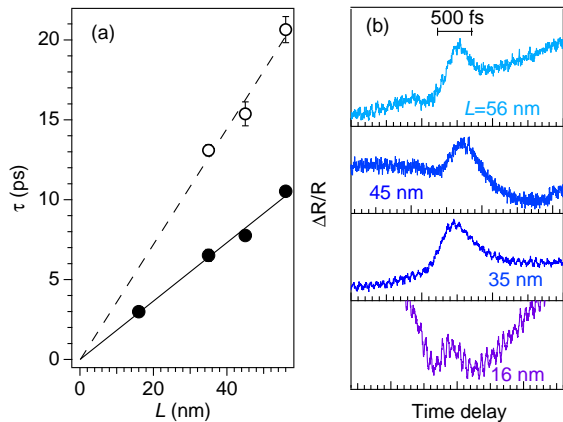


FIG. 3. (Color Online.) (a) Appearance times τ_1 and τ_2 of the first and second reflectivity spikes (filled and open circles) as a function of the GaP film thickness L . Lines represent linear fits. (b) Expanded reflectivity traces showing the first spikes.

schematically shown in Fig. 1. We also see smaller and broader spikes in the reflectivity at $\tau_2 \simeq 2\tau_1$ except for the thinnest ($L=16$ nm) film, whose arrival times are indicated by broken lines in Fig. 2a and by open symbols in Fig. 3a. We attribute the second spike to the acoustic pulse generated at the GaP/air surface and detected after a round trip in the GaP layer, which we have left out in the schematic in Fig. 1 for simplicity.

The most intriguing feature of the acoustic spike is its extremely short (~ 0.5 ps) temporal width of the acoustic pulse, as shown in Fig. 3b. The temporal width translates to a spatial extent of ~ 3 nm or ~ 10 atomic GaP bilayers. This is surprising because it is significantly smaller than the GaP film thickness or the optical penetration depths in GaP or Si, which would usually define the spatial extent of an acoustic pulse [18, 30].

IV. THEORETICAL MODELING AND DISCUSSION

We theoretically model the optical generation and detection of an acoustic pulse at a thin film of GaP of thickness L on a Si substrate, in the similar manner as in our previous study on bulk GaP and Si [23]. We consider the generation only via the deformation potential interaction, because the contribution of the thermoelastic effect is estimated to be an order of magnitude smaller in both GaP and Si [23]. We express the stress σ by the sum of the elastic component that is proportional to the strain $\eta \equiv \partial u / \partial z$ and the carrier density-dependent component:

$$\sigma(z, t) = \rho(z)v^2(z)\eta(z, t) - a_{cv}(z)N(z, t). \quad (1)$$

Here $\rho(z)$ is the mass density, and a_{cv} is the relative deformation potential coupling constant, defined by the

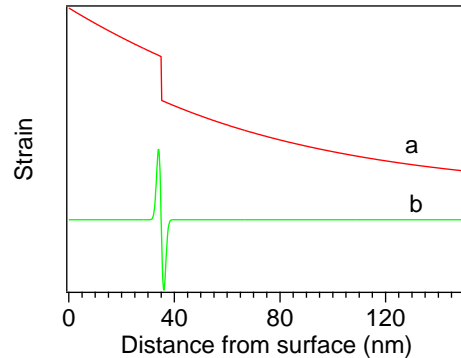


FIG. 4. (a) Calculated depth-profile of the initial strain induced by a carrier distribution expressed by eq. (2) (a) for $L=35$ nm. (b) Depth-profile of the bipolar strain pulse. Traces are offset for clarity.

difference between the coupling constants a_c and a_v of the conduction and valence bands. $N(z, t)$ denotes the photoexcited carrier density depending on the distance from GaP surface z and time t . We neglect the decay of the photoexcited carriers on the time scale in question and approximate $N(z, t) = 0$ for $t < 0$ and $N(z, t) = N(z)$ for $t \geq 0$.

We assume a heterointerface with GaP and Si maintaining their bulk electronic and optical and elastic properties, and neglect the contributions of the interfacial electronic states and band bendings at the interface. We express the carrier density by:

$$N(z) = \begin{cases} N_0 e^{-\alpha_{\text{GaP}} z} & \text{for } 0 \leq z \leq L \\ N_0 e^{-\alpha_{\text{GaP}} L} (1 - R_{\text{Si}}) \alpha_{\text{Si}} e^{-\alpha_{\text{Si}} (z-L)} & \text{for } z > L \end{cases} \quad (2)$$

where $N_0 = F(1 - R_{\text{GaP}})\alpha_{\text{GaP}}/\hbar\omega$ is the carrier density at $z = 0$, with F denoting the pump fluence, $\hbar\omega$, the pump photon energy, α_{GaP} and α_{Si} , the absorption coefficients in GaP and Si, and R_{GaP} and R_{Si} , the reflectivities at the GaP/air surface and at the GaP/Si interface. We solve the equation of elasticity by separating the time-independent and time-dependent components of the solution [31]. The obtained strain has an exponentially decaying depth profile with a kink at $z = L$, as shown in Fig. 4a for $L=35$ nm. The kink propagates in both GaP and Si directions with time, whereas another kink moves from the GaP surface ($z = 0$) into the GaP layer. The kinks are partially reflected and partially transmitted when they hit the GaP/Si and GaP/air boundaries.

We then calculate the dielectric constant and differential complex reflection coefficient in a thin film on a substrate following Ref. [31]. We approximate that the strain modifies the energy gap of the semiconductor and thereby introduces a shift in the dependence of the dielectric constant on the probe photon energy E [32]:

$$\frac{\partial \epsilon}{\partial \eta} \simeq -a_{cv} \frac{\partial \epsilon}{\partial E}. \quad (3)$$

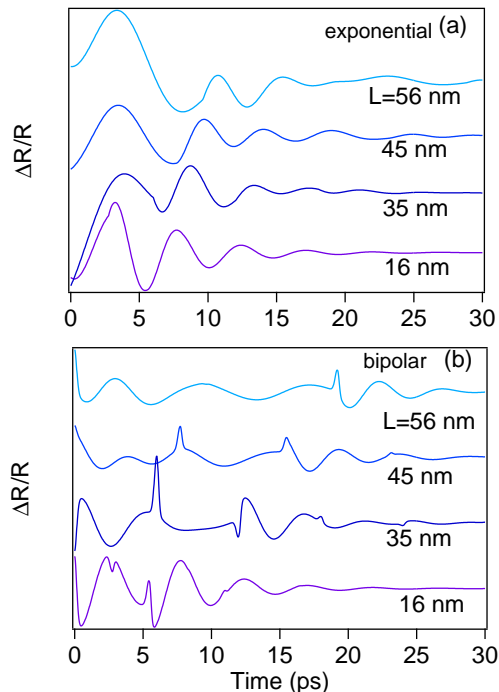


FIG. 5. Calculated reflectivity changes $\Delta R/R$ induced in GaP layer of different thickness L on Si by the exponentially decaying strain (a) and by the bipolar strain (b) whose initial profiles are shown in Fig. 4.

Figure 5a shows the reflectivity change $\Delta R/R$ calculated for different L . The traces feature nearly periodic oscillations that fail to reproduce the complicated phase jumps of the experiments. Moreover, the sharp spike at $t = L/v_{\text{GaP}}$ is almost invisible in the calculated reflectivity change, though our model allows the surface and interface to move when the strain pulse arrives, and thereby includes its effect on the reflectivity. Indeed, the absence of the sharp spike is consistent with the relatively long duration (tens of ps) of the calculated strain pulse, which is roughly estimated to be $2\alpha^{-1}v^{-1}$.

The discrepancy between the experiments and calculations suggests optical generation of much shorter strain pulse, which is not included in the above formulation. Because we do not see the sharp pulse in the reflectivity for bulk GaP or Si, we expect the generation to occur at the GaP/Si interface. To confirm this we assume an ultrashort bipolar strain pulse, whose initial depth profile is shown in Fig. 4b and calculate $\Delta R/R$ induced by it. The calculated reflectivity change, shown in Fig. 5b, reproduces the experimental quasi-periodic oscillations with phase jumps and spikes relatively well for $L=16, 45$ and 56 nm, if we change the sign. For $L=35$ nm, however, the agreement between the calculation and experiment is poorer.

Comparison of the experiments and calculations

strongly suggests that the ultrashort bipolar strain pulse generated at the GaP/Si interface dominates the reflectivity changes. In our theoretical modeling we assumed that the electronic bands are flat at the interface. At the actual interface, however, it is highly likely that the bands are bent in the vicinity of the interface and induce built-in electric field. In this situation, photoexcited electrons and holes would be separated quickly to the GaP and Si sides of the interface, where the deformation potential coupling constants of the conduction and valence bands do not cancel due to the charge imbalance.

The ultrashort duration (~ 3 nm or 0.5 ps) of the acoustic pulse observed in the present study has no match among the previous studies, even including those on metallic transducers designed specially to generate ultrashort acoustic phonons [19, 20]. In case of our GaP/Si samples, the strain pulse is created exclusively at the interface of the two semiconductors because the absorption coefficient α is different and, as a result, the photoexcited carrier density $N(t)$ has a step at the interface. The short duration of the acoustic pulse can be realized primarily by the nearly atomically abruptness of the GaP/Si interface, where the intermixing of GaP and Si atoms is limited to $\lesssim 7$ atomic layers [25]. The limited carrier diffusion in GaP (and Si) [23], compared with in metals and even in GaAs, also minimizes the expansion of the acoustic pulse duration during the propagation on the picosecond time scale.

V. CONCLUSION

We have reported the generation and detection of ultrashort acoustic pulses generated at the atomically flat GaP/Si(001) interface. The extremely narrow width of the strain pulse is due to the discontinuity of the photoexcited carrier density at the GaP/Si interface. The arrivals of the acoustic pulse at the surface are detected as sharp spikes in transient reflectivity. The acoustic pulses propagating in the GaP film and in the Si substrate are also detected as the quasi-oscillation in the reflectivity due to the photoelastic effect. Our abrupt interface translates into extreme acoustic temporal widths such as have not been achieved in other materials.

ACKNOWLEDGMENTS

This work is partly supported by the Deutsche Forschungsgemeinschaft through SFB 1083 and HO2295/8, as well as by NSF grant DMR-1311845 (Petek) and DMR-1311849 (Stanton).

-
- [1] C. Thomsen, H. Grahn, H. Maris, and J. Tauc, *Phys. Rev. B* **34**, 4129 (1986).
- [2] Y. Sugawara, O. Wright, O. Matsuda, M. Takigahira, Y. Tanaka, S. Tamura, and V. Gusev, *Phys. Rev. Lett.* **88**, 185504 (2002).
- [3] I. Lisiecki, D. Polli, C. Yan, G. Soavi, E. Duval, G. Cerullo, and M.-P. Pileni, *Nano Lett.* **13**, 4914 (2013).
- [4] J. Clark, L. Beitra, G. Xiong, A. Higginbotham, D. Fritz, H. Lemke, D. Zhu, M. Chollet, G. Williams, M. Messerschmidt, B. Abbey, R. Harder, A. Korsunsky, J. Wark, and I. Robinson, *Science* **341**, 56 (2013).
- [5] H. Ogi, M. Fujii, N. Nakamura, T. Yasui, and M. Hirao, *Phys. Rev. Lett.* **98**, 195503 (2007).
- [6] F. Hudert, A. Bruchhausen, D. Issenmann, O. Schecker, R. Waitz, A. Erbe, E. Scheer, T. Dekorsy, A. Mlayah, and J.-R. Huntzinger, *Phys. Rev. B* **79**, 201307 (2009).
- [7] A. Lomonosov, A. Ayouch, P. Ruello, G. Vaudel, M. Baklanov, P. Verdonck, L. Zhao, and V. Gusev, *ACS Nano* **6**, 1410 (2012).
- [8] M. Lejman, G. Vaudel, I. Infante, P. Gemeiner, V. Gusev, B. Dkhil, and P. Ruello, *Nat Commun* **5**, 5301 (2014).
- [9] C.-K. Sun, Y.-K. Huang, J.-C. Liang, A. Abare, and S. DenBaars, *Appl. Phys. Lett.* **78**, 1201 (2001).
- [10] J.-W. Kim, M. Vomir, and J.-Y. Bigot, *Sci. Rep.* **5**, 8511 (2015).
- [11] K. O'Brien, N. Lanzillotti-Kimura, J. Rho, H. Suchowski, X. Yin, and X. Zhang, *Nat. Commun.* **5** (2014).
- [12] R. Koehl and K. Nelson, *J. Chem. Phys.* **114**, 1443 (2001).
- [13] O. Wright and K. Kawashima, *Phys. Rev. Lett.* **69**, 1668 (1992).
- [14] G. Tas, J. Loomis, H. Maris, A. Bailes, and L. Seiberling, *Appl. Phys. Lett.* **72**, 2235 (1998).
- [15] M. Hettich, K. Jacob, O. Ristow, C. He, J. Mayer, M. Schubert, V. Gusev, A. Bruchhausen, and T. Dekorsy, *Appl. Phys. Lett.* **101**, 191606 (2012).
- [16] S. Kashiwada, O. Matsuda, J. Baumberg, R. Voti, and O. Wright, *J. Appl. Phys.* **100**, 073506 (2006).
- [17] T. Dehoux, O. Wright, R. Voti, and V. Gusev, *Phys. Rev. B* **80**, 235409 (2009).
- [18] O. Wright, B. Perrin, O. Matsuda, and V. Gusev, *Phys. Rev. B* **64**, 081202 (2001).
- [19] Q. Li, K. Hoogeboom-Pot, D. Nardi, M. Murnane, H. Kapteyn, M. Siemens, E. Anderson, O. Hellwig, E. Dobisz, B. Gurney, R. Yang, and K. Nelson, *Phys. Rev. B* **85**, 195431 (2012).
- [20] T. Dehoux, K. Ishikawa, P. Otsuka, M. Tomoda, O. Matsuda, M. Fujiwara, S. Takeuchi, I. Veres, V. Gusev, and O. Wright, *Light Sci Appl.* **5**, e16082 (2016).
- [21] V. Temnov, C. Klieber, K. Nelson, T. Thomay, V. Knittel, A. Leitenstorfer, D. Makarov, M. Albrecht, and R. Bratschitsch, *Nat Commun* **4**, 1468 (2013).
- [22] K. Volz, A. Beyer, W. Witte, J. Ohlmann, I. Nemeth, B. Kunert, and W. Stolz, *J. Crystal Growth* **315**, 37 (2011).
- [23] K. Ishioka, A. Rustagi, U. Höfer, H. Petek, and C. Stanton, *Phys. Rev. B*, submitted (2016).
- [24] A. Beyer, J. Ohlmann, S. Liebich, H. Heim, G. Witte, W. Stolz, and K. Volz, *J. Appl. Phys.* **111**, 083534 (2012).
- [25] A. Beyer, A. Stegmüller, J. Oelerich, K. Jandieri, K. Werner, G. Mette, W. Stolz, S. Baranovskii, R. Tonner, and K. Volz, *Chem. Mater.* **28**, 3265 (2016).
- [26] K. Ishioka, K. Brixius, U. Höfer, C. Stanton, and H. Petek, *Phys. Rev. B* **92**, 205203 (2015).
- [27] D. Aspnes and A. Studna, *Phys. Rev. B* **27**, 985 (1983).
- [28] K. Ishioka, K. Brixius, A. Beyer, A. Rustagi, C. Stanton, W. Stolz, K. Volz, U. Höfer, and H. Petek, *Appl. Phys. Lett.* **108**, 051607 (2016).
- [29] R. Weil and W. Groves, *J. Appl. Phys.* **39**, 4049 (1968).
- [30] E. Young, A. Akimov, R. Champion, A. Kent, and V. Gusev, *Phys. Rev. B* **86**, 155207 (2012).
- [31] O. Matsuda and O. Wright, *J. Opt. Soc. Am. B* **19**, 3028 (2002).
- [32] S. Adachi, *Phys. Rev. B* **35**, 7454 (1987); **38**, 12966 (1988).